ResearchGate

See discussions, stats, and author profiles for this publication at: https://www.researchgate.net/publication/315844203

Determination of Accurate Arrival Time of Meteotsunami Event in Yellow Sea

Conference Paper *in* Journal of Coastal Research · May 2017

DOI: 10.2112/SI79-031.1

CITATIONS
9

READS
154

6 authors, including:



Myung-Seok Kim
Korea Polar Research Institute (KOPRI)
22 PUBLICATIONS **91** CITATIONS
SEE PROFILE



Hyunsu Kim
Korea Power Exchange
46 PUBLICATIONS **127** CITATIONS
SEE PROFILE



Seung Buhm Woo
Inha University
108 PUBLICATIONS **874** CITATIONS
SEE PROFILE

All content following this page was uploaded by Hyunsu Kim on 10 April 2017.

The user has requested enhancement of the downloaded file.

Journal of Coastal Research	SI	79	149-153	Coconut Creek, Florida	2017

Determination of Accurate Arrival Time of Meteotsunami Event in Yellow Sea

Myung-Seok Kim[†], Hyunsu Kim[‡], Yoo-Keun Kim[‡], Sung-Hyup Yoo[§], Hyun-Min Eom[§], and Seung-Buhm Woo[†*]

[†]Department of Ocean Sciences
Inha University
Incheon, South Korea

[‡]Department of Atmospheric Sciences
Pusan National University
Busan, South Korea

[§]Marine Meteorology Division
Korea Meteorological Administration
Seoul, South Korea

www.cerf-jcr.org

www.JCRonline.org

ABSTRACT

Kim, M.-S.; Kim, H.; Kim, Y.-K.; Yoo, S.-H.; Eom, H.-M., and Woo, S.-B., 2017. Determination of accurate arrival time of meteotsunami event in Yellow Sea. *In:* Lee, J.L.; Griffiths, T.; Lotan, A.; Suh, K.-S., and Lee, J. (eds.), *The 2nd International Water Safety Symposium*. *Journal of Coastal Research*, Special Issue No. 79, pp. 149-153. Coconut Creek (Florida), ISSN 0749-0208.

According to a recent study by the Korean Meteorological Administration (KMA), unforeseen losses to property and human lives along the west coast of Korea in March 2007 were caused by meteotsunamis that originated at Shandong, which is located in eastern China. The determination of the arrival time of meteotsunamis in Yellow Sea is very important to protect human life and limit economic losses in coastal areas, because the analysis of meteotsunami propagation is primarily dependent on the method of arrival time. In this study, the meteotsunami event of March 29-31, 2007, the most powerful meteotsunami event reported in the Yellow Sea, was selected to find the optimal method of calculating the meteotsunami arrival time. It is difficult to estimate the arrival time of a meteotsunami that is commonly observed as a non-stationary signal in a time series without any specific criterion. To find a quantitative and reasonable method of estimating the arrival time, the propagation direction of the meteotsunami was analyzed using the arrival time at each tidal station derived from the absolute and relative threshold of the sea level oscillations in the meteotsunami frequency bands. The results indicated that the meteotsunami propagation derived using the relative threshold which defines the arrival time as the time when the amplitude of the sea level oscillation exceeds 3 standard deviations was more similar to the propagation pattern of the high rain rate field than other thresholds.

ADDITIONAL INDEX WORDS: *Meteotsunami, determination of the arrival time, propagation.*

INTRODUCTION

On March 31, 2007, an unexpected meteotsunami caused substantial damage to human lives and property along the southwest coast of South Korea. According to recent reports from the KMA, a total of 6 cases of damage due to the meteotsunami were reported. The first ever meteotsunami caused flooding on the west coast of Jeju Island on February 9, 2005 (Figure 1a), and a fisherman went missing near the GS coast on August 27, 2006 (Figure 1b). The meteotsunami on March 31, 2007, which generated the highest waves ever reported, injured 2 people and killed 4, and damaged property worth at least 2 million dollars by causing flooding in houses, destroying farms, overturning ships, and causing the flooding of the pumps of a nuclear power plant, which is located in YG (Figure 1c). The meteotsunami that occurred on May 4, 2008, recorded the severest damage to human life: 24 people near the coastal area were swept away (15 injured, 9 dead) by unexpected waves in BR (Figure 1d). On January 2, 2010, 1 person went missing because of the meteotsunami that propagated to Komun Island in the South Sea of Korea (Figure 1e). The successive harbor resonance after the meteotsunami in DH port on April 26, 2011 caused damage to property, including

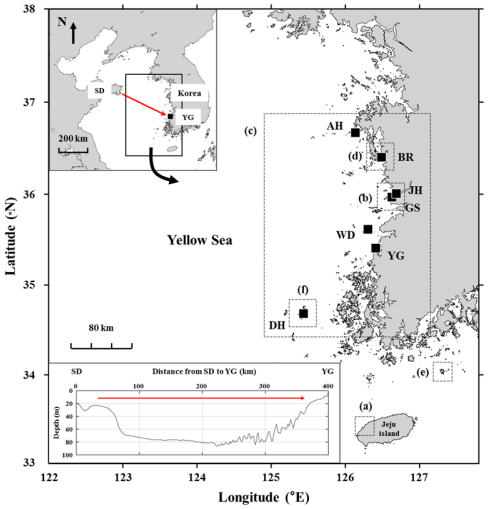


Figure 1. Map of the west coast of Korea showing the positions of the AnHeung (AH), BoRyeong (BR), JangHang (JH), GunSan (GS), WiDo (WD), YeongGwang (YG) and DaeHeuksando (DH) tidal stations. The red arrows indicate the depth transect of the meteotsunami which occurred on March 31, 2007, from Shandong (SD) to YeongGwang (YG). The gray dashed boxes enclose the area where accident occurred (a-f).

DOI: 10.2112/SI79-031.1 received 30 September 2016; accepted in revision 31 October 2016.
*Corresponding author: sbwoo@inha.ac.kr
©Coastal Education and Research Foundation, Inc. 2017

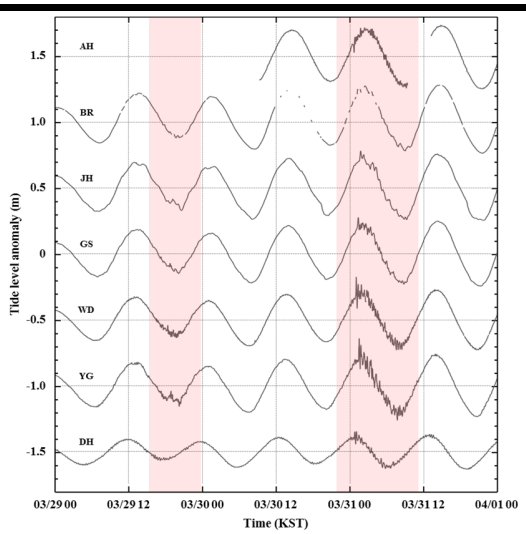


Figure 2. Tide level anomaly from north to south. Red rectangular (shaded) boxes indicate the meteotsunami events that occurred on March 29 and 31, 2007.

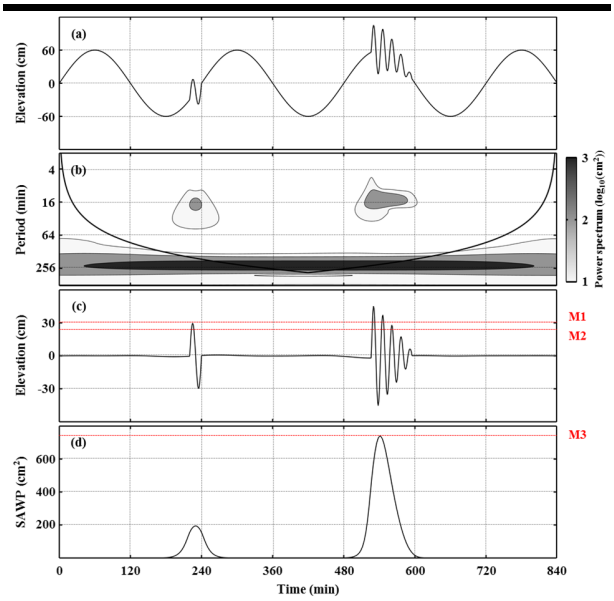


Figure 3. Methods of determining the arrival time of the meteotsunami with the artificial time series (M1-M3); (a) Nonstationary time series similar to the tide level on March 31, 2007. (b) Wavelet spectra of the time series. The contour intervals are 10 cm^2. The parabolic line indicates the "cone of influence", where edge effects become important. (c) High-pass filtered (2 h) time series. (d) Scale Averaged Wavelet Power (SAWP) of the high-pass filtered time series.

the destruction of the cage system, losses of fish farms and flooding of small ships (Figure 1f).

To date, previous studies in Korea have mainly focused on the cause of the events of March 31, 2007, and May 4, 2008, which caused the greatest damage, with somewhat insufficient focus on the prevention of disasters. In order to send warnings about the propagation direction of the meteotsunami and the resulting danger zones in the future, precise criteria that enable the arrival time of meteotsunamis along the west coast of Korea to be determined are required. The methods of determining the arrival time of meteotsunamis can be roughly categorized as criteria using absolute thresholds, relative thresholds, and alternative thresholds, the last of which uses both the absolute and relative thresholds. If the sea level change in the Ciutadella inlet exceeds 30 cm, Rabinovich and Monserrat (1996) selected the absolute threshold, which determines the meteotsunami arrival time uniformly. However, because such an absolute threshold does not consider the level of background noise for each region, Monserrat, Vilibić, and Rabinovich (2006) suggested using a relative threshold which considers the arrival to occur when the occurrence amplitude exceeds 3 or 4 standard deviations for any given region.

In order to select the most reasonable method of determining the arrival time of meteotsunamis in the Yellow Sea, this study carried out a comparative analysis of the arrival time according to each of the methods suggested by preliminary studies on the meteotsunami event of March 29-31, 2007. Of these different methods, the one that gave the most precise direction of meteotsunami propagation was selected as the optimal method.

METHODS

Among the methods of determining the arrival time suggested by the preliminary studies, 3 types of methods using the absolute and relative thresholds of the amplitude and power spectrum were compared. Method M1 uses an absolute threshold, which defines the time point where the amplitude in the meteotsunami frequency bands exceeds 30 cm as the meteotsunami arrival time, regardless of the region. Method M2 uses a relative threshold, which varies according to the region, and defines the time point where the amplitude in the meteotsunami frequency bands exceeds 3 standard deviations for the first time as the meteotsunami arrival time. Method M3 also uses a relative threshold that defines the time point where the Scale-Averaged Wavelet Power (SAWP) of the sea level oscillations in the meteotsunami frequency bands is the highest as the meteotsunami arrival time. Due to the characteristics of the meteotsunami signal that appears as a type of nonstationary group wave rather than a solitary wave, it may be better to consider the power spectrum of the wave group in the meteotsunami frequency bands, unlike in methods M1 and M2. By using the SAWP, which is the weighted sum of the wavelet power spectrum in a specific frequency band, the fluctuation of the corresponding wave group as it varies with time can be examined (Torrence and Compo, 1998).

To select the optimal method among the 3 methods, a comparative analysis of the propagation of the meteotsunami derived using each method was performed. The rain rate, which is one of the atmospheric instability factors, was used to estimate the precise direction of meteotsunami propagation. Using the rain rate displayed on the radar image at 10 min intervals, the temporal and spatial distributions of the clusters of rain can be identified. Kim *et al.* (2016) shows that the

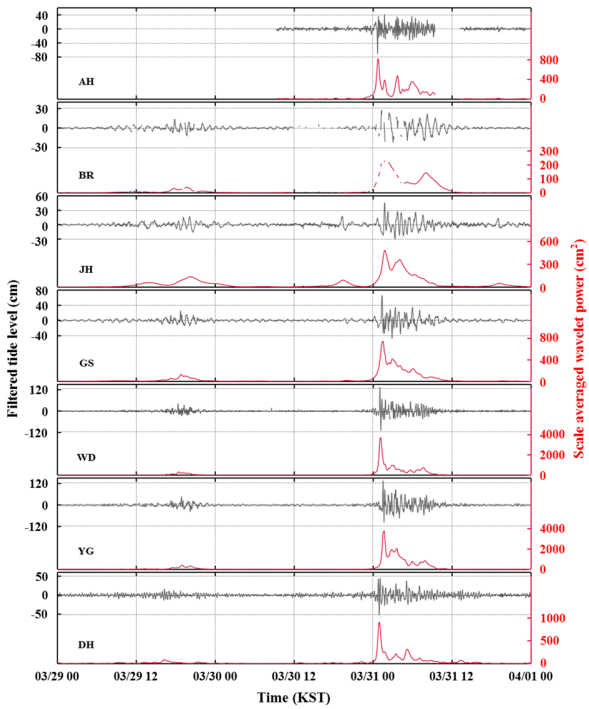


Figure 4. High-pass filtered (2 h) tide level and Scale Averaged Wavelet Power (SAWP) of the filtered tide level. AH and BR tide level data which had too many missing data during the meteotsunami events were high-pass filtered after linear interpolation.

propagation of the meteotsunami event of March 29-31, 2007, showed a similar pattern to the evolution of the high rain rate. Therefore, the correspondence between the clusters of high rain rate (more than 5 mm/h) that occurred before the meteotsunami and the propagation direction of the meteotsunami determined by each arrival time method were qualitatively investigated. The direction of meteotsunami propagation was analyzed using the algorithm for the estimation of the meteotsunami propagation (Kim, Woo, and Eom, 2013), which utilizes the order of the arrival time, the arrival time difference between each tidal station, and the shallow water wave speed equation.

RESULTS

As shown in Figure 2, a total of 2 meteotsunami events occurred, one during low tide on March 29, 2007, and the other during high tide on March 31, which occurred due to the consecutive eastward movement of the pressure jump from SD to YG (Choi, Park, and Kwon, 2008). When the meteotsunami occurred, tsunami-like waves were dominantly observed in the high frequency bands, and different ranges of sea level oscillations were recorded at each tidal station. To identify the characteristics of each method under ideal conditions, an artificial time series that is similar to the tide level during meteotsunamis at YG was constructed (Figure 3a). In the artificial time series, the meteotsunami component which is characterized by localized peaks, the damping peaks that

Table 1. *Meteotsunami arrival time derived from each method on March 29 and 31, 2007.*

Date	Station	Arrival Time (HH:MM)		
		M1	**M2**	**M3**
March 29, 2007	AH	-	-	-
	BR	-	17:46	19:45
	JH	-	19:07	20:13
	GS	-	17:15	18:48
	WD	18:20	17:19	18:25
	YG	18:50	17:16	18:57
	DH	-	16:09	16:15
March 31, 2007	AH	00:38	00:38	00:44
	BR	-	01:14	01:57
	JH	01:41	01:41	01:47
	GS	01:17	01:17	01:28
	WD	00:59	01:00	01:07
	YG	01:19	01:27	01:40
	DH	00:46	00:45	00:56

dissipated non-periodically in the high frequency bands, and one tidal component which is a stationary signal in the low frequency bands, were superposed. The artificial meteotsunami component was constructed using the high frequency waves shorter than 2 hours, which are within the range of the meteotsunami frequency bands (Rabinovich and Monserrat, 1996).

To extract the meteotsunami component from the artificial time series and the observed tide level, the evolution of the power spectrum with the time and frequency was first identified by using the wavelet transform (Figure 3b), and the sea level oscillations in the meteotsunami frequency bands were high-pass filtered with a Butterworth filter (Figure 3c). After extracting the meteotsunami components from the artificial time series, each method of determining the arrival time (M1-M3) was analyzed to check when the arrival time was defined, respectively.

When threshold M1 was applied, regardless of the magnitude of the amplitude, the arrival time was determined at 30 cm. The arrival time obtained by method M2 was generally defined as being before the occurrence of the daily maximum amplitude (Figure 3c), and the threshold was applied differently according to time and space. The arrival time of method M3 was defined as being after the daily maximum amplitude had occurred, at the latest time when the wave height was the highest (Figure 3d). When the amplitude of the meteotsunami was less than 30 cm, the arrival time was not determined by method M1, as in the case of the March 29, 2007 event, when the meteotsunami amplitude was relatively small and the arrival time could not be specified with method M1, because all regions except for WD and YG showed a low amplitude less than the M1 threshold (Figure 4, Table 1). On March 31, 2007, the meteotsunami was detected by method M1 in all regions except for BR, and it moved southeastward from the eastern area of the Yellow Sea in the order of AH, HS, WD, GS, YG, and JH (Table 1, Figure 5b1). Method M1, which disregards the when locality of the specific region, could not detect the arrival time the sea level oscillated at a lower amplitude than the M1 threshold, such as in BR (Table 1).

When M2 and M3, which are relative threshold methods, are applied, the arrival time can be obtained in all regions and at

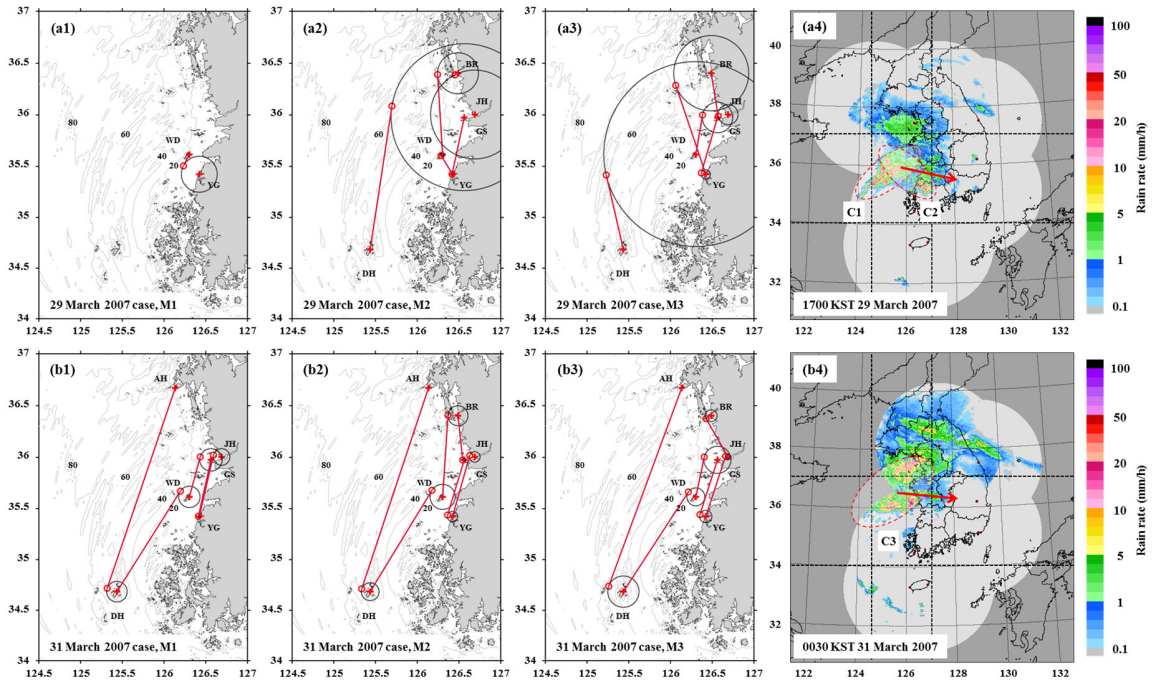


Figure 5. Meteotsunami propagation determined by each arrival time method (a1-a3, b1-b3) derived from the propagation algorithm of the meteotsunami (Kim, Woo, and Eom, 2013) and radar image showing the rain rate which can represent the approximate propagation of the meteotsunami (a4, b4 red dashed ellipses and red arrows) on March 29 and 31, 2007. The red cross marks indicate each tidal station at which the meteotsunami occurred when using each arrival time method. The thick red line is the wave crest line of the meteotsunami. The radius of each black circle, which represents the distance from the red cross mark to the point of tangency, is the distance the meteotsunami moved. The gray lines are bathymetric contours in Yellow Sea (20-80 m).

all times. As seen on the artificial time series, the arrival time of M2 was also earlier than that of M3 in the raw time series (Table 1). The sea level variations in BR oscillated with extremely low amplitude during the meteotsunamis (Figure 2, Figure 4) and there was a much longer time lag between the arrival times of M2 and M3 in BR compared to the other tidal stations (Table 1). In particular, for the event of March 29, 2007, which was a relatively small scale meteotsunami, the time lag between the arrival times of M2 and M3 was considerable (1 h-2 h) in all tidal stations except for HS, which is located in the outermost region (Table 1). Moreover, when M2 was applied to the meteotsunami on March 29, 2007, the meteotsunamis propagated southeastward along the west coast of Korea, but, on the contrary, when M3 was applied, they propagated northeastward (Figure 5a2-a3), Table 2). When disregarding the arrival order of BR, the meteotsunamis on March 31, 2007 propagated southeastward and finally concentrated in the GS-YG region at an average speed of 23 m/s (Figure 5b2-b3, Table 2).

DISCUSSION

As a meteotsunami propagates to all tidal stations, sea level oscillations may vary from one site to another as shown in Figure 2 and Figure 4 although it is generated by the same mechanism. It might be more appropriate to use a relative threshold method (M2, M3), which reflects the regional locality of each tidal station, than the absolute threshold. Methods M2 and M3 can be applied to the meteotsunami on March 31, 2007 because it is by now well known that the meteotsunamis occurred in all regions (Eom *et al.*, 2012). Methods M2 and M3 are only applicable at a given meteotsunami date and in the case of powerful meteotsunamis which can propagate to most of the tidal stations. It is necessary to modify these 2 methods when analyzing the arrival time of meteotsunamis which are not known or occurred locally in specific regions. An alternative threshold method, which applies the absolute and relative thresholds simultaneously, can detect the arrival time even for the numerous minor cases that occur below the relative threshold (Monserrat, Vilibić, and Rabinovich, 2006). To search for the minor cases in terms of the magnitude of meteotsunamis, the absolute threshold in the alternative threshold method must represent the level of background noise at all tidal stations. Therefore, the alternative threshold method requires the sea level data in all regions during sufficiently long periods of time and robust statistical analysis to support the basis of the absolute

Table 2. *Meteotsunami propagation derived from each method on March 29 and 31, 2007.*

Date	Propagation Direction					
	M1		**M2**		**M3**	
	Case	Slope* (deg)	Case	Slope* (deg)	Case	Slope* (deg)
March 29, 2007	WD-YG	60.6	HS-GS	79.3	HS-WD	-79.1
	-	-	GS-YG	76.4	WD-GS	78.9
	-	-	YG-WD	-60.1	GS-YG	72.3
	-	-	WD-BR	-88.0	YG-BR	-72.9
	-	-	BR-JH	25.0	BR-JH	-82.2
	-	-	-	-	-	-
March 31, 2007	AH-HS	69.3	AH-HS	69.7	AH-HS	67.8
	HS-WD	55.9	HS-WD	56.7	HS-WD	55.0
	WD-GS	73.3	WD-BR	84.6	WD-GS	76.5
	GS-YG	75.9	BR-GS	-85.3	GS-YG	70.7
	YG-JH	75.5	GS-YG	71.7	YG-JH	70.4
	-	-	YG-JH	72.8	JH-BR	-61.5

*Slope of the wave crest line is measured counter clockwise from the eastward direction.

threshold. Considering the advantages and disadvantages of each arrival time method practically, it can be appropriate to use the current relative threshold method with minor revisions.

The direction of propagation of the meteotsunami derived from method M2 showed the most similar pattern to that of the rain rate in the March 29-31, 2007 event among the 3 methods (Figure 5a2, a4, b2, b4). Of the clusters of rain rates on March 29, 2007, C2 dissipated during propagation and only C1 moved southeastward along the coast (Figure 5a4). This result is the most similar to the direction of meteotsunami propagation derived from method M2 (Figure 5a2). The propagation direction derived from method M3 was different from that of method M2 (Figure 5a2-a3), Table 2) because of the overestimated arrival time difference between the tidal stations (Table 1, Table 2). In the case of the March 29, 2007 meteotsunami event, the maximum SAWP occurrence time (M3) after the first run-up (M2) was considerably delayed at all tidal stations. These time lags also varied with the region, and the arrival order of methods M2 and M3 also varied (Table 1). It seemed that the time lags due to getting longer time difference between the time point when meteotsunami arrived first and the time point when successive harbor resonance occurred after the meteotsunami in the case of relatively small-magnitude meteotsunamis (Figure 4). However, all of the propagation results derived from methods M1, M2, and M3 for March 31, 2007, were very similar to the propagation of C3 (Figure 5b1-b4), Table 2).

Method M2 detected the arrival times of the meteotsunamis at all times and in all regions, because the levels of background noise in each region were determined as the standard deviation of the daily amplitude sample in the meteotsunami frequency bands. Furthermore, another disadvantage of method M2 is that the standard deviation is changed in every day. Therefore, it is necessary to compute the standard deviation for the yearly or long-term amplitude sample instead of the daily amplitude sample. It is expected that even the arrival times of meteotsunamis that occur with a relatively small intensity will be able to be detected with the modified M2 method. In the near future, if the propagation result can be estimated in advance by applying a lower threshold than 3 standard deviations in the outer region, it can be utilized as a meteotsunami warning system.

CONCLUSIONS

It is concluded here that the relative threshold method is an optimal method for arrival time of the meteotsunami based on the highly accurate result of meteotsunami propagation direction derived from the arrival time method. The arrival time is defined as particular point in time when the amplitude of the sea level oscillation in the meteotsunami frequency bands exceeds 3 standard deviations for the first time (M2). To detect even the arrival time of partially propagated meteotsunami events and unknown meteotsunami events, the long-term amplitude sample more than 1 day at each tidal station will be required. This arrival time method can be useful tool for preventing coastal hazards caused by meteotsunamis by issuing warning in advance at outer regions in Yellow Sea.

ACKNOWLEDGMENTS

This work was funded by the Korea Meteorological Administration Research and Development Program under Grant KMIPA 2015-1071. Additionally, this research was a part of the project titled ‘Manpower training program for ocean energy’, funded by the Ministry of Oceans and Fisheries, Korea.

LITERATURE CITED

Choi, B.J.; Park, Y.W., and Kwon, K.M., 2008. Generation and growth of long ocean waves along the west coast of Korea in March 2007. *Ocean and Polar Research*, 30(4), 453-466.

Eom, H.M.; Seung, Y.H.; Woo, S.B., and You, S.H., 2012. Analysis of abnormal wave at the west coast on 31 March 2007. *Journal of Korean Society of Coastal Ocean Engineers*, 24(3), 217-227.

Kim, M.S.; Woo, S.B., and Eom, H.M., 2013. Propagation of abnormal waves on 25 April 2008 at the West Coast of South Korea. *In:* Conley, D.C.; Masselink, G.; Russell, P.E., and O'Hare, T.J. (eds.), *Proceedings from the International Coastal Symposium (ICS) 2013* (Plymouth, United Kingdom). *Journal of Coastal Research*, Special Issue No. 65, pp. 731-735.

Kim, M.S.; Kim, H.; Kim, Y.K.; Gu B.H.; Lee H.J., and Woo S.B., 2016. Double Resonance Effect at Daeheuksando Port Caused by Air Pressure Disturbances in Yellow Sea on 31 March 2007. *In:* Vila-Concejo, A.; Bruce, E.; Kennedy, D.M., and McCarroll, R.J. (eds.), *Proceedings from the International Coastal Symposium (ICS) 2016* (Sydney, Australia). *Journal of Coastal Research*, Special Issue No. 75, pp. 1142-1146.

Monserrat, S.; Vilibić, I., and Rabinovich, A.B., 2006. Meteotsunamis: atmospherically induced destructive ocean waves in the tsunami frequency band. *Natural Hazards Earth System Sciences*, 6, 1035-1051.

Rabinovich, A.B. and Monserrat, S., 1996. Meteorological tsunamis near the Balearic and Kuril Islands: Descriptive and statistical analysis. *Natural Hazards*, 13(1), 55-90.

Torrence, C. and Compo, G.P., 1998. A practical guide to wavelet analysis. *Bulletin of the American Meteorological Society*, 79, 61-78.

View publication stats